

Studies on hardness and tensile testing of AlSi10Mg produced by Selective Laser Melting

¹Krishna C, ¹Kushal Kumar H G, ¹Shiva Kumar K M, ¹Suraj M, ²Shreyas P S

School of Mechanical Engineering, REVA University

Abstract— The present paper systematically investigated the influence of solution heat treatments on mechanical properties of SLM-produced AlSi10Mg alloy parts. Due to the high cooling rate of SLM the internal stress which gives rise to significantly better tensile properties and Vickers micro-hardness. The variation in size of the Si particles has a significant influence on the mechanical properties of the AlSi10Mg samples. The tensile strength decreases from 433.25 MPa for the as-built sample to 166.11 MPa, while the fracture strain remarkably increases from 5.30% to 23.7% when the as-built sample is solution-treated at 550°C for 2 h. This study indicates that the mechanical properties of SLM-processed AlSi10Mg alloy can be tailored by suitable solution and artificial aging heat treatments.

Index Terms— AlSi10Mg, Density, Mechanical properties, Heat treatment, Selective Laser melting(SLM),

1 INTRODUCTION

Selective laser melting (SLM) is layer-based additive manufacturing technology that is utilized to manufacture complex and customized structures from metal powder. The main advantage of this process over conventional manufacturing methods is the facility to create lightweight parts. SLM saves resources, reduce waste and carbon footprint [1], [2]. SLM also makes it possible to manufacture parts from materials that can be difficult to machine [3], such as AlSi10Mg, which, due to the presence of the hard Si phase, is mainly used in casting.

AlSi10Mg alloy, a hypoeutectic alloy in the Al-Si-Mg system, is highly demanded for many applications in aerospace, automotive industries and heat exchange and recycling costs, and high mechanical properties[4]. It is well known that the morphology and size of eutectic silicon are the two most important factors significantly affecting the mechanical properties of AlSi10Mg alloy [5]. McDonald et al. [6] revealed that coarse and acicular eutectic silicon phases initiate cracks in the tension environment, which deteriorates mechanical properties. Therefore, it is imperative that the modification of coarse and acicular eutectic silicon phases is made to improve the mechanical properties of AlSi10Mg alloy for the ever-growing application demands in aerospace and other fields[7]. There have been a number of previous studies concerned with parameter optimization to produce close to fully dense parts from Al alloy using SLM, such as [8], [9], [10]. The use of High laser power (up to 1 KW) was recommended by Buchbinder et al. [11]. The manufacture of load bearings parts using SLM is being considered in numerous application and consequently, the mechanical performance of SLM parts is gaining further attention. SLM of Al alloys produce a characteristically fine microstructure [12] that has been shown to yield mechanical behavior significantly different from that seen in conventionally cast material [13], which usually has a coarser microstructure. There are several aspects that require consideration when studying the mechanical behavior of SLM parts. Although the effect of build orientation has been reported as influential on the tensile properties of Ti alloys

[14], it has less influential in the case of AlSi10Mg; mainly elongation under tensile loading [13], [14]. The energy density delivered to the material during processing also affects the mechanical properties. Various mechanical properties of SLM parts made from Al alloy have been reported in the literature, such as tensile behavior [13], [14], [15] impact resistance, and fatigue performance showed that the tensile strength of SLM AlSi10Mg is higher than that of the die cast counterpart, but the latter has better ductility. [16] investigated the effect of the energy density, build plate preheating, and post processing stress relief on the tensile properties of SLM AlSi12, reporting that the energy density had the strongest influence. [17] reported a higher hardness for SLM AlSi10Mg when compared to the die-cast equivalent as well as improved impact resistance.

Selective laser melting (SLM), as an emerging technology of additive manufacturing (AM), is a powder bed fusion process, which is capable of producing metal components with complex free-form geometries directly from three-dimensional (3D) computer-aided design (CAD) data [18], [19]. The laser energy is absorbed by powder particles complying with the complex coupling mechanisms between the laser and the materials, such as laser-bulk coupling and laser-powder coupling, when the high energy laser beam is radiated on powder [16]. Due to the transient interaction between the laser beam and the powder bed, a high temperature gradient (up to 105 °C/m) and a rapid cooling rate (up to 106–108 °C/s) occurs in the SLM process [20]. Therefore, the SLM process possessing extremely rapid solidification and a high cooling rate has great potential for the modification of the eutectic silicon phase in Al-Si-Mg alloys. The processing parameters of the SLM process have a substantial effect on the refinement of eutectic silicon and resultant mechanical properties of as-built AlSi10Mg components.

Recently, some efforts have been made to study the AlSi10Mg alloy manufactured by SLM. [21] studied the TiC/Al-Si10Mg nanocomposites migration behavior and mechanism during SLM, and found that the particle size of TiC/AlSi10Mg varied from standard nanoscale structure to

the relatively coarsened submicron morphology with the increase of laser energy per unit length. [22] studied the physical mechanism of the hydrogen pores in AlSi10Mg parts manufactured by SLM, and the hydrogen porosity could be lowered by the efficient drying of the powder as well as modification the process parameters of SLM. Qiu et al. [23] elaborated on the influence of processing conditions on strut structure and compressive properties of cellular lattice structures fabricated by selective laser melting. He discovered that the specific yield strength of AlSi10Mg is dependent of SLM processing conditions, indicating that further improvement in properties of AlSi10Mg can be achieved by process optimization. Kempen et al. [24] focused their attentions on the optimization of SLM process parameters for building nearly fully dense AlSi10Mg parts. The as-built AlSi10Mg parts exhibit excellent mechanical properties like ultimate tensile strength owing to the very fine microstructure, but the elongation is relatively lower compared to the high pressure die cast counterparts.

Alloying magnesium to the Al-Si alloy enables the precipitation of Mg₂Si phase, which significantly improves ductility and strengthens the matrix without compromising other mechanical properties. AlSi10Mg can be hardened through the precipitation of Mg₂Si phase by a specified T6 heat treatment (solution with complete artificial aging) [25]. Currently, there were some pre-liminary studies on the heat treatments of as-processed SLM Al-Si10Mg parts. Brandl et al. [25] studied the microstructure, high cycle fatigue, and fracture behavior of as-built and peak-hardened treatment of SLM AlSi10Mg samples. They found that post heat treatment has the more considerable effect on the fatigue resistance of AlSi10Mg than building direction, and also the fatigue limit and static tensile strength significantly correlate with the size and morphology of eutectic silicon. Aboulkhair et al. [26] investigated the solution heat treatment and aging duration time on micro-hardness of SLM-processed AlSi10Mg. As far as the authors' knowledge, few work has systematically studied on the eutectic silicon evolution and mechanical properties of SLM-made Al-Si10Mg parts when subjected to heat treatment.

Therefore, in the present paper, a systematically investigation has been conducted on the influence of solution and artificial aging on the eutectic and mechanical properties of SLM-produced AlSi10Mg alloy parts.

2. EXPERIMENTAL DETAILS

2.1 AlSi10Mg Specimens Fabricated by SLM

AlSi10Mg tensile bars shown in Figure. 1 were fabricated on a EOSINT M 280 facility (RAPID DMLS, Bengaluru). The SLM machine is equipped with a 400 W Gaussian beam fiber laser with a focal laser beam diameter of 80 μ m. The processing parameters have been optimized as follows: the laser power was 350 W, laser scan speed was 1140 mm/s, the powder layer thickness was 50 μ m and the scan spacing was 170 μ m. The SLM production was performed in an inert argon atmosphere to avoid the pick-up of interstitial oxygen (lower than 0.2%). The AlSi10Mg parts were cut from the Al substrate using wire electrical discharge machining after production. It is worth noting that the substrate was heated to 100 $^{\circ}$ C for the purpose

of reducing internal stress during the SLM process.

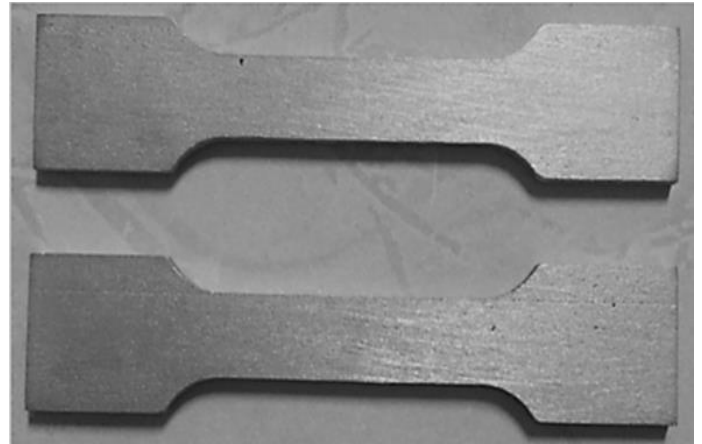


Fig: 1 Tensile specimens of AlSi10Mg alloy made by SLM.

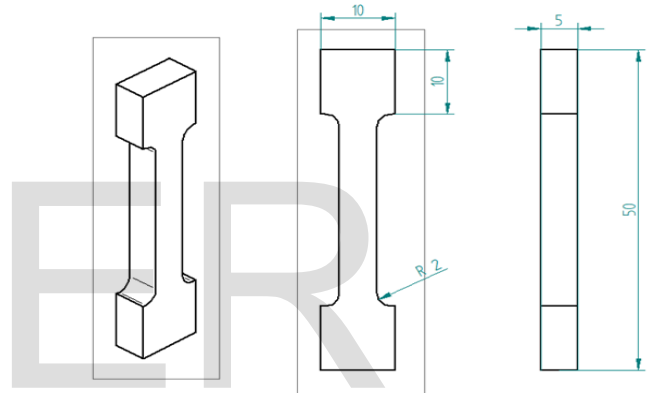


Fig: 2 Dimensions of the specimen

2.2 Heat treatment of SLM- produced AlSi10Mg Specimens

In accordance with the standard T⁶ heat treatment process, the SLM-produced AlSi10Mg specimens were solution-treated at the different temperatures of 450 $^{\circ}$ C, 500 $^{\circ}$ C and 550 $^{\circ}$ C for 2 h, followed by water quenching. After the solution heat treatment, one half of the specimens were immediately subjected to artificial aging at 180 $^{\circ}$ C for 12 h, and then all the samples were equally water quenched to room temperature [25], [26].

2.3 Mechanical Properties of the specimens

The tensile strength of the AlSi10Mg specimens before and after the heat treatments were characterized by a high-precision electronic universal testing machine (AG-100kN, Shimadzu, Japan) with a constant strain rate of 1 mm/min. The tensile specimen is illustrated in Fig. 1. Vickers hardness tests were carried out on a 430SVD hardness test machine (Wilson Hardness, America) at a load of 1000 gf and a loading time of 15 s. Before mechanical properties testing, all of the test specimens were polished with a 2000 # sand paper to remove the surface layer (e.g. oxidations, contaminations), which would impose a negative influence

3.RESULTS AND DISCUSSION

3.1 Mechanical Properties

The tensile stress-strain curves obtained from the room temperature tensile testing on the as-built and different solution heat-treated AlSi10Mg specimens are shown in Fig. 3 (a). The variations of the tensile strength, yield strength and ductility with the solution temperature are given in Fig. 3 (b). The as-built SLM specimen exhibits the highest tensile and yield strengths of 434.25 MPa and 322.17 MPa, respectively, but possesses a lowest ductility of 5.370.22%. The solution heat treatment has a great influence on the mechanical properties of the SLM made AlSi10Mg specimens. As the sample is solution heat-treated at 450 °C for 2 h, there is a dramatic decrease in both tensile and yield strengths (282.3676.1 MPa and 196.5873.6 MPa, respectively), whilst a large increase in ductility of 13.470.51% can be observed. With further increase of the solution temperature up to 500 °C, the tensile and yield strengths are reduced to 213.7574.6 MPa and 126.00 MPa respectively, and the ductility increases to 23.570.81%. However, when the solution temperature reaches 550 °C, the specimens exhibit the lowest tensile and yield strengths (168.11 MPa and 90.52 MPa, respectively), while the ductility slightly increases to the maximum (23.770.84%). For the specimens subjected to both solution heat treatment and artificial aging at 180 °C for 12 h, the mechanical properties are shown in Fig. 3 (c). it can be found that the ultimate strength and ductility both decrease with the increase in the solution temperature. The tensile strength decreases from 197.11 MPa to 187.14 MPa, while the ductility decreases from 23.370.87% to 19.570.69%, as the solution temperature increased from 500 °C to 550 °C. The high strength of the as-built SLM AlSi10Mg specimens can be attributed to the grain refinement. The effect of grain size on the mechanical properties can be rationalized by the semi-empirical Hall-Petch (HP) relationship[27], [28], [29], which is indicated in "(1)":

$$\sigma = \sigma_0 + kd^{-1/2} \tag{1}$$

where σ is the proof stress, σ_0 is the friction stress for dislocation movement, k is the Hall-Petch coefficient, and d is the grain size. The size-induced strengthening results from the pile-up of dislocations at grain boundaries as well as resistance of the dislocations to slip transfer. Grain size refinement leads to reduction of the distance between the Si particles, which can give a considerable contribution to the strength because the increased Al-Si interface can effectively reduce the movement of dislocations. Moreover, due to the nano-sized eutectic network Si in the as-built AlSi10Mg sample, the localized shear stress can be relieved and hence increase the strength. The strength and ductility after heat treatment

are influenced by many factors, such as number, morphology and size of the Si phases, initial hardening rate and recovery rate [30]. The last two factors are closely related to the solute content in the solid solution. Upon solution and artificial aging, the Si atoms trapped in the Al matrix are rapidly precipitated out onto the existing eutectic network Si, thus reducing the solid solution strengthening. Meanwhile, the distance between the Si particles increases significantly, which also contributes to the decreased of tensile and yield strengths. As to the ductility of the as-built SLM samples and solution heat-treated specimens in this study, two aspects need to be considered. Firstly, the decrease in the number of Si particles and increase in size induce the reduction of localized stress or strain. Secondly, solution heat treatment reduces the residual stresses that are built up during the SLM process. These two aspects benefit the enhancement of the ductility of the solution heat-treated AlSi10Mg specimens. However, due to the over aging effect, the ductility decreases after the artificial aging.

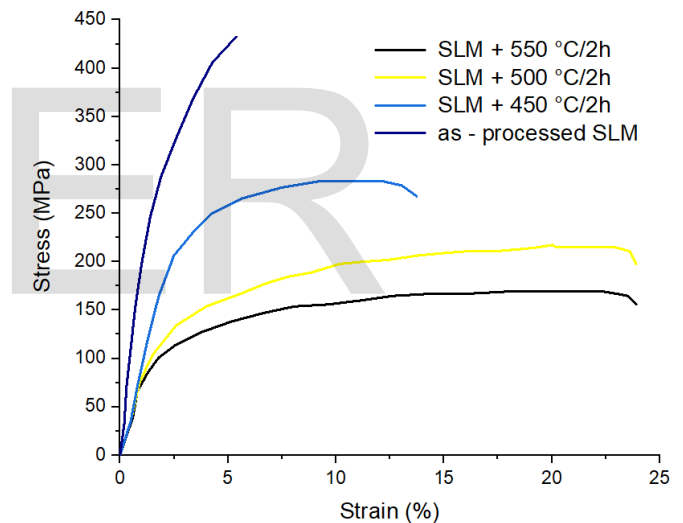


Fig. 3 (a). Room temperature tensile stress-strain curves of the as-built SLM samples that solution heat-treated at different temperatures.

Hardness is also an important indicator for the material's capability to resist plastic deformation [31]. In order to evaluate the influence of heat treatment on the hardness of the as-built SLM AlSi10Mg specimens, Vickers micro-hardness is introduced and the corresponding results are illustrated in Fig. 3(d). In general, the hardness values of the heat-treated specimens are lower than the those of the as-built ones. Due to the fine dispersion of eutectic Si in the Al matrix, the as-built AlSi10Mg SLM specimens have the maximum micro-hardness value, namely 132.55 Hv₁. After the solution treatment at 450 °C for 2 h, a

ISSN 2229-5518
 Significant decrease in micro-hardness can be observed (95.65 Hv₁). When the solution treatment temperature is further increased from 500 °C to 550 °C, the micro-hardness decreases from approximately 87.85 Hv₁ to 63.55 Hv₁. It is worth noting that artificial aging also has a negative effect on the micro-hardness of the samples that have been subjected to the solution treatment. After the artificial aging at 180 °C for 12 h, the micro-hardness further reduces to 78.15 Hv₁, 60.55 Hv₁ and 52.5 Hv₁ for the specimens that have been solution heat-treated at 450°C, 500 °C and 550 °C, respectively, as illustrated in the red bars in Fig. 4(d). This behavior is in a good agreement with the evidence found in the tensile tests. This result can be also attributed to the coalescence of small Si particles as well as Ostwald ripening, which result in an increase in size and decrease in the number of particles.

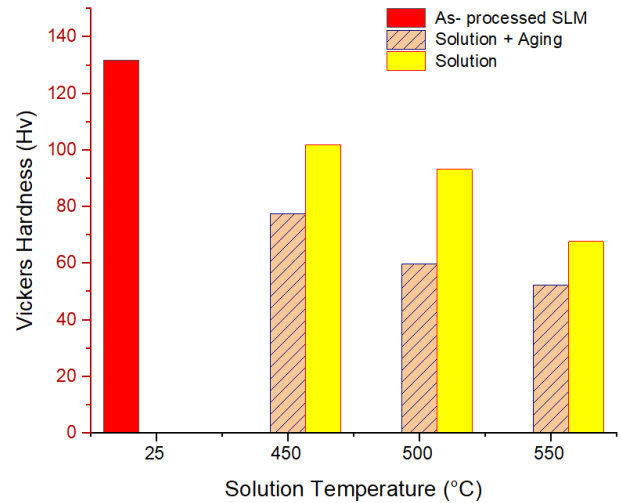


Fig. 3 (d). the Vickers hardness of the as-built and heat-treated SLM specimens.

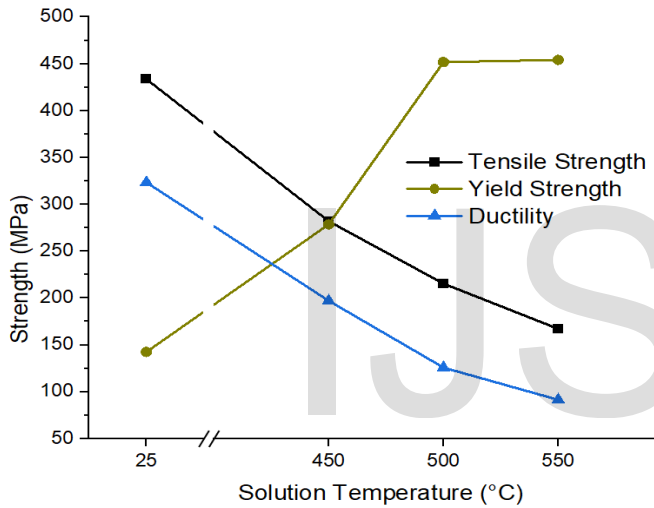


Fig. 3 (b). corresponding mechanical data.

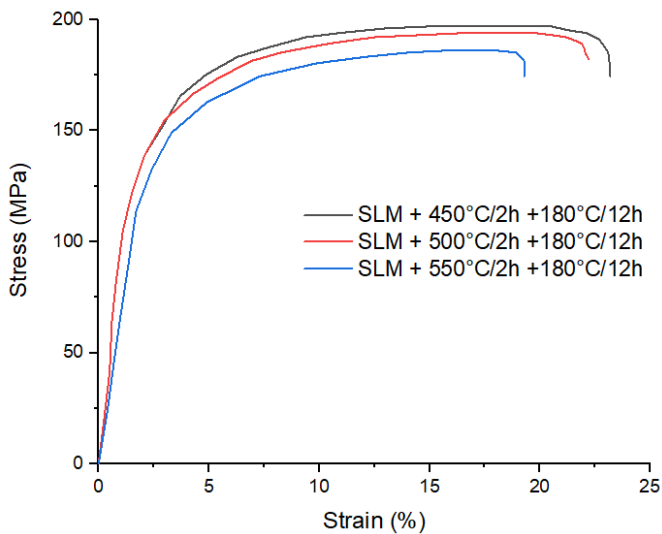


Fig. 3 (c). tensile test stress-strain curves of the solution + artificial aging specimens.

4 CONCLUSION

In this study, the effects of the solution and artificial aging heat treatments on the phase, mechanical properties of the SLM-produced AlSi10Mg specimens are systematically studied. The main results and findings are as follows.

- The as-received SLM parts was very brittle because of the residual stress developed during the processing
- The solutionized sample was much softer than the as received sample. Hence we can conclude that the residual stresses developed during processing was relieved from the solutionizing heat treatment.
- As the solutionizing temperature was decreasing the strength & hardness found to be decreasing. Hence from our studies we can conclude that depending on the ductility required we have to choose the solutionizing temperature.

Summarizing all the results of the research and observation, it should be noted that the SLM technology gives wide range of possibilities to manufacture complex-shape structures and components. However, to achieve high mechanical properties the parameters should be selected properly, to avoid high porosity, which is mainly responsible for the properties of tested material.

6 REFERENCES

[1] A. Aremu, I. Ashcroft, R. Wildman, R. Hague, C. Tuck, D. Brackett, Proc. Inst. Mech. Eng. B: J. Eng. Manuf. (2013).
 [2] N. Gardan, Int. J. Manuf. Eng. 2014 (2014) 9.

- [3] A. Gebhardt, F.-M. Schmidt, J.-S. Hotter, W. Sokalla, P. Sokalla, *Phys. Procedia* 5 (B) (2010) 543-549.
- [4] B. Li, H.W. Wang, J.C. Jie, Z.J. Wei, Effects of yttrium and heat treatment on the microstructure and tensile properties of Al-7.5Si-0.5Mg alloy, *Mater. Des.* 32 (2011) 1617-1622.
- [5] Y.C. Tsai, C.Y. Chou, S.L. Lee, C.K. Lin, J.C. Lin, S.W. Lim, Effect of trace La addition on the microstructures and mechanical properties of A356 (Al-7Si-0.35Mg) aluminum alloys, *J. Alloy. Compd.* 487 (2009) 157-162.
- [6] S.D. McDonald, K. Nogita, A.K. Dahle, Eutectic nucleation in Al-Si alloys, *Acta Mater.* 52 (2004) 4273-4280.
- [7] X.P. Li, X.J. Wang, M. Saunders, A. Suvorova, L.C. Zhang, Y.J. Liu, M.H. Fang, Z. H. Huang, T.B. Sercombe, A selective laser melting and solution heat treatment refined Al-12Si alloy with a controllable ultrafine eutectic microstructure and 25% tensile ductility, *Acta Mater.* 95 (2015) 74-82.
- [8] K. Kempen, L. Thijs, J. Van Humbeeck, J.P. Kruth, *Mater. Sci. Technol.* 31(2014) 917-923.
- [9] N.T. Aboulkhair, N.M. EVERITT, I. ASHCROFT, C. Tuck, *Addit. Manuf.* 1-4 (2014) 77-86.
- [10] S. Dadbakhsh, L. Hao, P.G.E. Jerrard, D.Z. Zhang, *Powder Technol.* 231(2012) 112-121.
- [11] D. Buchbinder, H. Schleifenbaum, S. Heidrich, W. Meiners, J. Bültmann, *Phys. Procedia* 12(A)(2011)271-278.
- [12] L. Thijs, K. Kempen, J.P. Kruth, J. Van Humbeeck, *Acta Mater.* 61(2013) 1809-1819.
- [13] N. Read, W. Wang, K. Essa, M.M. Attallah, *Mater. Des.* 65 (2015) 417-424.
- [14] M. Simonelli, Y.Y. Tse, C. Tuck, *Mater. Sci. Eng.: A* 616 (2014) 1-11.
- [15] X.J. Wang, L.C. Zhang, M.H. Fang, T.B. Sercombe, *Mater. Sci. Eng.: A* 597 (2014) 370-375.
- [16] S. Siddique, M. Imran, E. Wycisk, C. Emmelmann, F. Walther, *J. Mater. Process. Technol.* 221 (2015) 205-213.
- [17] K. Kempen, L. Thijs, J. Van Humbeeck, J.P. Kruth, *Phys. Procedia* 39 (2012) 439-446.
- [18] S. Zhang, Q.S. Wei, L.Y. Cheng, S. Li, Y.S. Shi, Effects of scan line spacing on pore characteristics and mechanical properties of porous Ti6Al4V implants fabricated by selective laser melting, *Mater. Des.* 63 (2014) 185-193.
- [19] Q.S. Wei, S. Li, C.J. Han, W. Li, L.Y. Cheng, L. Hao, Y.S. Shi, Selective laser melting of stainless-steel/nano hydroxyapatite composites for medical applications: microstructure, element distribution, crack and mechanical properties, *J. Mater. Process. Technol.* 222 (2015) 444-453.
- [20] Y.L. Li, D.D. Gu, Parametric analysis of thermal behaviour during selective laser melting additive manufacturing of aluminium alloy powder, *Mater. Des.* 63 (2014) 856-867.
- [21] P.P. Yuan, D.D. Gu, D.H. Dai, Particle migration behavior and its mechanism during selective laser melting of TiC reinforced Al matrix nano composites, *Mater. Des.* 82(2015)46-55.
- [22] C. Weingarten, D. Buchbinder, N. Pirch, W. Meiners, K. Wissenbach, R. Poprawe, Formation and reduction of hydrogen porosity during selective laser melting of AlSi10Mg, *J. Mater. Process. Technol.* 221(2015) 112-120.
- [23] C.L. Qiu, S. Yue, N.J.E. Adkins, M. Ward, H. Hassanin, P.D. Lee, P.J. Withers, M. M. Attallah, Influence of processing conditions on strut structure and compressive properties of cellular lattice structures fabricated by selective laser melting, *Mater. Sci. Eng.* A628(2015)188-197.
- [24] K. Kempen, L. Thijs, J.V. Humbeeck, J.P. Kruth, Processing AlSi10Mg by selective laser melting: parameter optimisation and material characterization, *Mater. Sci. Technol.* 31(2015)917-923.
- [25] E. Brandl, U. Heckenberger, V. Holzinger, D. Buchbinder, Additive manufactured AlSi10Mg samples using Selective Laser Melting (SLM): microstructure, high cycle fatigue, and fracture behavior, *Mater. Des.* 34 (2012) 159-169.
- [26] N.T. Aboulkhair, C. Tuck, I. Ashcroft, I. Maskery, N.M. Everitt, On the precipitation hardening of selective laser melted AlSi10Mg, *Metall. Mater. Trans. A* 46A (2015) 3337-3341.
- [27] M.R. Basariya, V.C. Srivastava, N.K. Mukhopadhyay, Microstructural characteristics and mechanical properties of carbon nanotube in forced aluminum alloy composites produced by ball milling, *Mater. Des.* 64 (2014) 542-549.
- [28] Y.Z. Zhu, S.Z. Wang, B.L. Li, Z.M. Yin, Q. Wan, P. Liu, Grain growth and micro-structure evolution based mechanical property predicted by a modified Hall-Petch equation in hot worked Ni76Cr19AlTiCo alloy, *Mater. Des.* 55 (2014) 456-462.
- [29] X.H. Dong, X.T. Hong, F. Chen, B.R. Sang, W. Yu, X.P. Zhang, Effects of specimen and grain sizes on compression strength of annealed wrought copper alloy at room temperature, *Mater. Des.* 64 (2014) 400-406.
- [30] Y. Chen, M. Weyland, C.R. Hutchinson, The effect of interrupted aging on the yield strength and uniform elongation of precipitation-hardened Al alloys, *Acta Mater.* 61(2013)5877-5894.
- [31] D. Buchbinder, H. Schleifenbaum, S. Heidrich, W. Meiners, J. Bültmann, High power selective laser melting (HPSLM) of aluminum parts, *Phys. Procedia* 12 (2011) 271-278

IJSER

IJSER